JOURNAL OF MATERIALS SCIENCE 12 (1977) 2109–2114

The relationship between the occurrence of twin-related laths and the fracture elongation in the two-phase (α+γ) Fe-Cr-Ni stainless steel

K. WAKASA, T. NAKAMURA
Department of Metallurgical Engineering, Tokyo Institute of Technology, O-okayama, Meguro-ku, Tokyo, Japan.

The relationship between the occurrence of twin-related laths and fracture elongation has been studied in two-phase ($\alpha + \gamma$) Fe–Cr–Ni stainless steel. The percentage of adjacent twin-related lath martensites increased as the deformation temperature increased from −196 to −50° C. The appearance of these twin-related laths, having the accommodation effect, contributed to the increase in elongation.

1. Introduction

A packet martensite consists of blocks or bundles of lath-shaped crystals. The blocks are separated by high-angle boundaries, but the groups of parallel laths within each block are separated by relatively low-angle boundaries. This type of microstructure has been observed in quenched Fe–Ni alloys [1, 2], Fe–C alloys [3, 4], Fe–Cr–Ni stainless steel [6], and other iron-base alloys containing Sn, V, W, Mo and Pt [7]. There often appears a twin relationship between adjacent laths within a block. The proportion of such twins increases with the transformation temperature and approaches 100% in a two-phase ($\alpha + \gamma$) Fe–Cr–Ni stainless steel transformed at −50° C [8]. Furthermore, this high twin probability corresponds to a peak in the elongation of the specimen if the tensile direction is parallel to the rolling direction [9].

In the present study, transmission electron microscropy was used to measure the percentage of twin-related laths formed in the temperature range between −196 and −50° C, and this was correlated with the elongations of sheet specimens having tensile directions at various angles to the rolling direction.

2. Experimental procedure

The material tested was the two-phase ($\alpha + \gamma$) Fe–Cr–Ni alloy, containing (wt%) 23.19% Cr, 4.91% Ni, 0.025% C, 1.47% Mo, 0.53% Si, 0.51% Mn, 0.91% Al, 0.023% P and the balance Fe. The sheets were cut at the angles of 0°, 45° and 90° to the rolling direction, and machined into tensile specimens having an 18.0 mm gauge length, a thickness of 2.0 mm and a test section width of 6.0 mm. They were annealed for 1 h at 1000° C, and the resultant mean grain size of the α- and γ-phase was approximately 8.0 μm. From light microscope observation, it was found that the proportion of γ-phase was 52%.

Tensile testing was carried out using an Instron type testing machine operating at a cross-head speed of 0.5 mm $min.^{-1}$ Specimens were tested in the temperature range between −196 and 26° C. The integrated X-ray intensities of $(1\,1\,1)_\gamma$, $(2\,0\,0)_\gamma$, $(2\,2\,0)_\gamma$, $(1\,1\,0)_\alpha$ $(2\,0\,0)_\alpha$ and $(2\,1\,1)_\alpha$ diffraction peaks were measured as a function of the amount of deformation in order to monitor the proportion of α' martensite which formed during tensile testing [8]. This proportion was also measured from light micrographs. Finally, the transformation structures and the orientation relationship between martensite laths were studied by transmission electron microscopy.

3. Experimental results

3.1. The appearance of a peak temperature

A peak appears in the elongation–test temperature

curve of metastable austenitic steels [10, 11], and this phenomenon depends on the occurence of the martensite transformation during straining. Furthermore, it is found that it depends on both the delay of the start of necking and the suitable value of α' martensite per unit tensile strain in a sheet tensile specimen having tensile direction parallel to the rolling direction [9]. Thus, it is necessary to clarify the temperature-dependence of fracture elongation in other tensile specimens having tensile directions of 45° and 90° to the rolling direction.

Fig. 1 shows the variation of the fracture elongation in 0°-, 45°- and 90°-specimens with test temperature. The Ms temperature of γ-phase was around −196° C, and the Md* in the fractured specimen was approximately −22° C. The peak occurred in the fracture elongation between Ms and Md temperatures for these tensile specimens. The peak temperature was −50° C in the 0°- and 45°-specimens. In a 90°-specimen, the peak elongation appeared at both −102 and −50° C. Therefore, the TRIP† effect was found in these tensile specimens. A difference occurred in the values of fracture elongation; the elongation was larger at the 0°- and 45°-specimens than at the 90°-specimen in the temperature range −196 to 22° C. The increase in the elongation depending on the martensite transformation did not appear above −22° C, because the α'-phase did not form during form during straining above this temperature.

The peak elongation depended on the amount of α' per unit tensile strain, as pointed out previously [9], and this was measured in case of the 45°- and 90°-specimens. Fig. 2 shows the relationship between the amount of α' martensite per unit tensile strain and the fracture elongation in the 0°-, 45°- and 90°-specimens. The elongations varied linearly with the amount of α' per unit strain at each test temperature: the larger this amount was, the larger the elongation. As already reported by the authors, the elongation in the 0°-specimen had the maximum value at −50° C, the amount of α' per unit strain being 0.68. This result was also found in the 45°- and 90°-specimens. At the peak temperature, corresponding to the maximum value of fracture elongation, the amounts of α' per unit strain in 0°-, 45°- and 90°-specimens were 0.26, 0.58 and 0.68, respectively.

* Martensite formed by tensile deformation.
† Transformation-induced plasticity

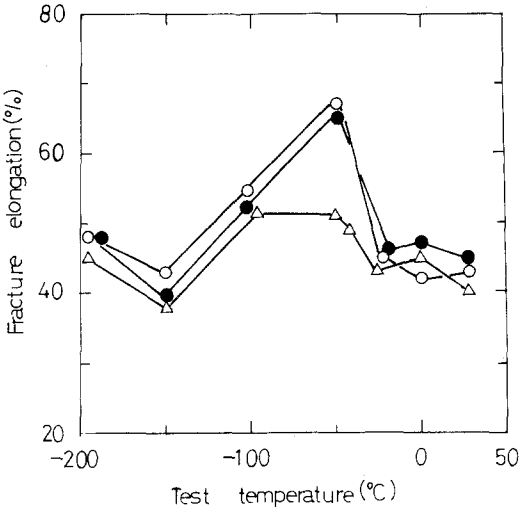

Figure 1 The temperature-dependence of fracture elongation in tensile specimens having tensile directions of 0° ○, 45° ● and 90° △ to the rolling direction.

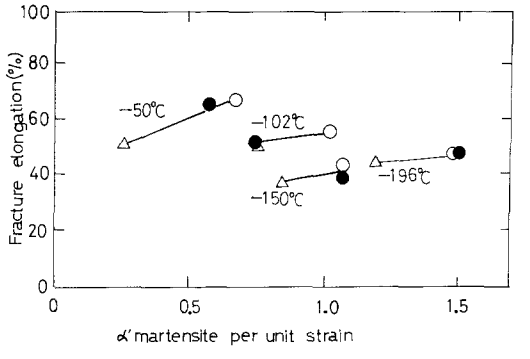

Figure 2 Relation between α' martensite per unit tensile strain and fracture elongation in ○ 0°-, ● 45°- and △ 90°-specimens in the temperature range −196 to −50° C.

3.2. The variation of the integrated intensity ratio in diffracted planes of α- and γ-phases with the amount of plastic deformation

As the martensite transformation occurs during straining, it is clear that the integrated intensities in diffracted planes of α- and γ-phases vary with tensile strain. Those measured were the $(1\,1\,0)_\alpha$, $(2\,0\,0)_\alpha$ and $(2\,1\,1)_\alpha$ planes in α-phase, and the $(1\,1\,1)_\gamma$, $(2\,0\,0)_\gamma$ and $(2\,2\,0)_\gamma$ planes in γ-phase. Fig. 3a, b and c show the variation of the integrated intensity ratio with the amount of tensile strain in deforming 0°-, 45°- and 90°-tensile specimens at −50° C, respectively. The ratio was obtained at six different diffracted planes of α- and γ-phases, and this is the proportion of the integrated intensity in the specimen deformed to a certain strain to

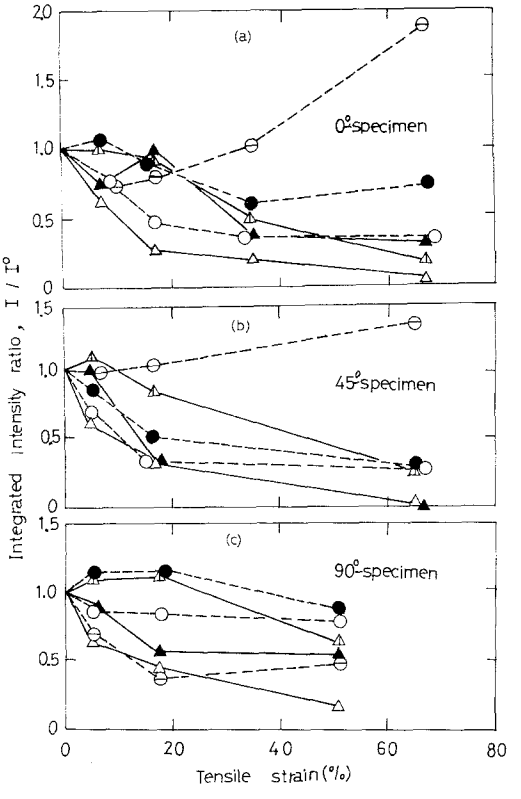

Figure 3 The variation of integrated intensity ratio with tensile strain in (a) 0°-, (b) 45°- and (c) 90°-specimens. The ratio is I/I° at respective diffracted-planes: I is the respective integrated intensity at $(1\,1\,1)_{\gamma}$, $(2\,0\,0)_{\gamma}$, $(2\,2\,0)_{\gamma}$, $(1\,1\,0)_{\alpha}$, $(2\,0\,0)_{\alpha}$ and $(2\,1\,1)_{\alpha}$ planes in the deformed specimen, and I° respective integrated intensity at those planes in an annealed specimen. △ $(1\,1\,1)_{\gamma}$, ▲ $(2\,0\,0)_{\gamma}$, ⏢ $(2\,2\,0)_{\gamma}$, ○ $(1\,1\,0)_{\alpha}$, ● $(2\,0\,0)_{\alpha}$, ⊖ $(2\,1\,1)_{\alpha}$.

that in the annealed specimen. The variation of this ratio may be equivalent to changing the integrated intensities in the planes parallel to the specimen surface. In Fig. 3a, b and c, their ratios in the $(1\,1\,1)_{\gamma}$, $(2\,0\,0)_{\gamma}$ and $(2\,2\,0)_{\gamma}$ planes of γ-phase decreased with increasing tensile strain. This tendency shows the occurrence of martensite transformation during plastic deformation, and the ratios in the diffracted planes of α-phase varied increasingly with strain. It follows that the α-martensite having planes parallel to the specimen surface increases with increasing deformation. A difference occurred among these variations of ratios with strain in 0°-, 45°- and 90°-specimens. In the 0°- and 45°-specimens, the ratio in $(2\,1\,1)_{\alpha}$ plane increased remarkably as the amount of strain increased. In case of a 90°-specimen, the ratio in $(2\,0\,0)_{\alpha}$ plane was larger than those in the $(1\,1\,0)_{\alpha}$ and $(2\,1\,1)_{\alpha}$ planes at fracture strain, while the ratio in the $(2\,1\,1)_{\alpha}$ plane decreased with increasing the amount of deformation. These results imply that the orientations of α' parallel to the specimen surface which increased with increasing the amount of strain were the $(2\,1\,1)_{\alpha}$ and $(2\,0\,0)_{\alpha}$ planes in 0°- or 45°-, and 90°-specimens, respectively.

The variations of the integrated intensity ratios with the amount of strain were also examined in 0°-, 45°-and 90°-specimens at −196, −150 and −102° C. The changes of $(2\,1\,1)_{\alpha}$ and $(2\,0\,0)_{\alpha}$ planes at these temperatures had the same features as those at −50° C in respective tensile specimens.

3.3. The occurrence of stress-induced α' martensite

α' martensite induced by a tensile stress occurs within the γ-phase of the Fe–Cr–Ni stainless steel. Fig. 4 shows the amount of α' martensite in deforming to failure 0°-, 45°- and 90°-specimens in temperature range −196 to −22° C. This amount increased with decreasing the test temperature, and between −150 and −50° C was larger in the 0°- and 45°-specimens than in the 90°-specimen. At −196° C, the austenite transformed completely to α'-martensite.

The tensile strains in 0°-, 45°- and 90°-specimens, where the α' martensite formed between −196 and −22° C, had the same value at respective deformation temperatures, and the values at −196, −150, −102, −50 and −22° C were below 1.0,

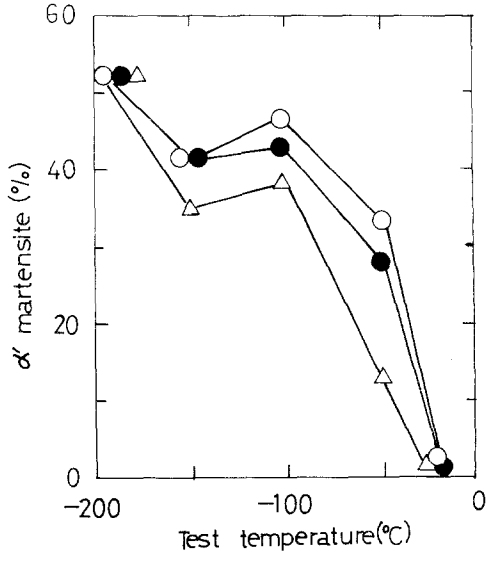

Figure 4 The temperature-dependence of amount of α'-martensite in ○ 0°-, ● 45°- and △ 90°-specimens.

~1.0, 5.0, 17.0 and 25.0%, respectively. The amount of α' that formed at various strains after the transformation was, however, different in respective tensile specimens. Thus, there appeared a difference among the values of α' martensite per unit tensile strain, as shown in Fig. 2.

The morphology of stress-induced martensite was the lath martensite in the temperature range between −196 and −22° C. Plate-like martensites with a mid-rib were not found the γ-phase of the present Fe–Cr–Ni alloy. As a martensite structure, there appeared some blocks within an original austenite grain, which were the groups of the laths. Fig. 5 shows the lath martensites formed in deforming to failure a 0°-specimen at −50° C :Fig. 5a is a bright field electron micrograph of a goup of parallel laths, and Fig. 5b is an electron diffraction pattern taken from the beam direction of $[\bar{3}\,1\,1]_\alpha$ at the boundary of two laths shown in a. Fig. 5c and d are the dark field images of the laths obtained at $(0\,1\,\bar{1})_\alpha$ and $(0\,1\,\bar{1})_t$ spots, respectively. From Fig. 5b, the orientation between them was seen to be in a twin relationship, and it follows that both groups of the laths shown in Figs. 5c and d are in the twin relationship. Thus it is necessary to examine the kind of the orientation relationships between the laths that are found at other temperatures. An orientation analysis was carried out on martensite structure formed during straining at −196, −150, −102 and −50° C, and the results are shown in Table I.

4. Discussion

4.1. Effect of orientation relationship between adjacent laths on fracture elongation between −196 and −50° C

The amount of lath martensite increases gradually with increasing plastic deformation, because the value of α' martensite per unit tensile strain is approximately constant during straining. As the laths form in the adjacent places, the orientation relationship between them might be expected to be specific. In fact, it is a twin orientation relationship [1, 2, 6, 8].

However, the amount of adjacent laths having twin relationship found between −196 and −50° C is not known. As the fracture elongation increases, depending upon the martensite transfromation during straining, it is useful to obtain the percentage of twin-related laths in this temperature range in order to clarify the relationship between martensite substructure and elongation.

Table I indicates the percentage of twin-related laths in case of a 0°-specimen observed in the temperature range −196 to −50° C. 8 kinds of diffraction pattern were observed at these temperatures. In $[\bar{3}\,1\,1]_\alpha$, $[1\,1\,0]_\alpha$ and $[1\,1\,1]_\alpha$ beam directions, twin spots formed for $\{1\,1\,2\}_\alpha$ twin-plane, so the relationship between adjacent laths was a twin relationship. The diffraction pattern indexed as $[1\,1\,3]_\alpha$ and $[1\,1\,0]_\alpha$ zones had an approximately twin relationship, i.e. ~5° off the twin relationship. The diffraction patterns of $[1\,1\,1]_\alpha$ and $[\bar{1}\,1\,3]_\alpha$ zones, $[1\,0\,2]_\alpha$ and $[\bar{1}\,\bar{1}\,1]_\alpha$ zones, and $[1\,1\,1]_\alpha$ and $[0\,1\,1]_\alpha$ zones or $[0\,0\,\bar{1}]_\alpha$ and $[1\,1\,0]_\alpha$ zones, were approximately 9°, 15°, and 19° off the twin relationship respectively. Their patterns did not belong to a group of twin-related laths. The temperature, where the orientation relationship between the laths is in a twin relationship, is equivalent to the peak temperature of a 0°-specimen. In 45°- and 90°-specimens, the peak temperature was −50° C, as shown in Fig. 1. From the above, it is deduced that there may be a twin relationship at the peak temperature. In order to investigate this, the orientation relationship in the 90°-specimen was analysed. The adjacent laths observed at −50° C in the 90°-specimen were in a twin relationship. Thus, the temperature-dependence of twin-related laths which are observed in

TABLE I Percentage of twin-related lath martensite in a 0°-specimen between −196 and −50° C. T = twin relationship between the laths; 5°, 9°, 15° and 19° show the deviation angles from the twin relationship, respectively. It is supposed that twin-related martensites are equivalent to martensites containing the twin relationship and a 5° deviation.

Test temperature (° C)	Number in sample	Orientation relationship and its number	Percent of twin-related lath martensite (%)
−50	25	T (25)	100
−102	22	T (16) 5° (2) 19° (4)	82
−150	18	T (8) 5° (4) 9° (5) 15° (1)	67
−196	22	T (9) 5° (5) 9° (4) 15° (3) 19° (1)	64

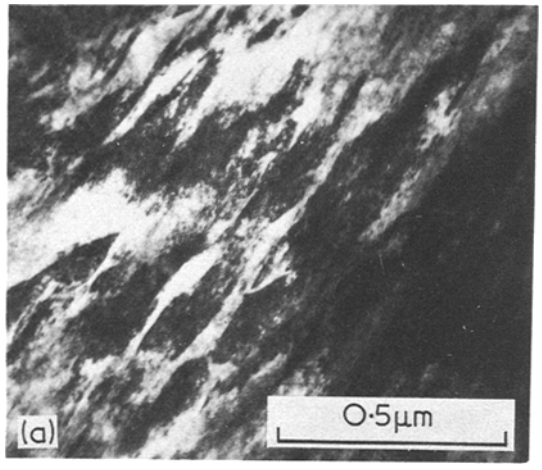

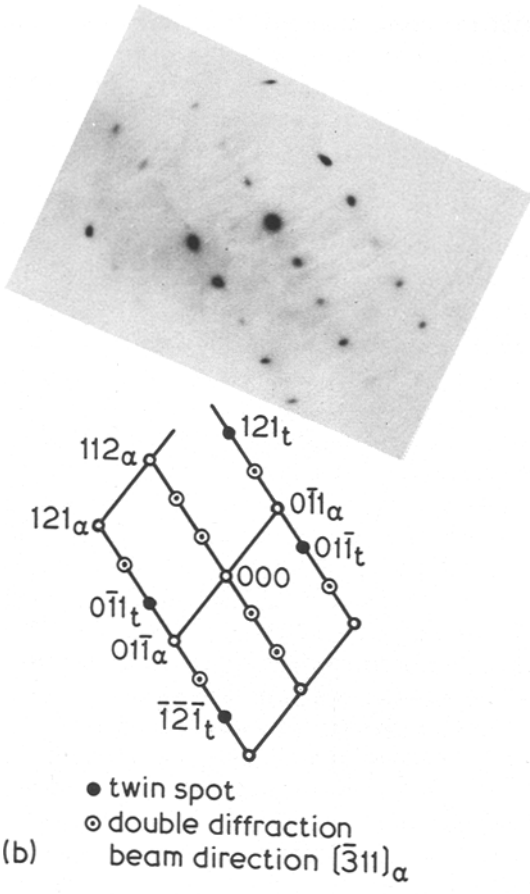

Figure 5 Transmission electron micrographs of lath martensites; (a) a bright field image of laths, (b) an electron diffraction pattern, (c) and (d) dark field images which are twin-related laths.

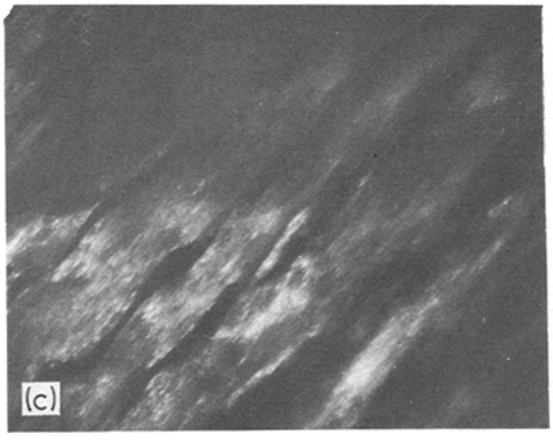

45°- and 90°-specimens at other temperatures may indicate the same tendency as the result obtained at a 0°-specimen. As shown in Fig. 1, the fracture elongation decreased with lowering the test temperature from −50 to −196° C and the percentage of the twin-related laths also decreased. This implies that the occurrence of these laths is related to the increase in fracture elongation.

The occurrence of the twin-related laths is considered as follows: these laths have shear components of respective strain in a shape deformation which are exactly opposite [12]. The orientation relationship between γ and the lath was the Kurdjumov–Sachs relationship in the case of the present Fe–Cr–Ni alloy. According to Speich and Swann [1], and Chilton *et al.* [4], they indicate

that the occurrence of both the twin-related laths and the laths separated by low- or high-angle boundaries is expected if the adjacent regions of laths have different variants of Kurdjumov–Sachs relationship. This agreed with the present experimental observations given in Table I. The strain in the shape deformation is a shear on the $(\bar{1}\,\bar{1}\,2)_\gamma$ habit plane in the $[\bar{1}\,1\,0]_\gamma$ direction plus an expansion normal to the habit plane. In case of twin-related laths are observed. As the shear components of the strains in the shape deformation cancel in this case, the strains tend to accommodate there. Thus, the strain energy obtained in the occurrence of twin-related laths is minimized [12]. Combinations of other variants which are off the twin relationship do not show the accommodation effect. This orientation relationship between them was found at three different test temperatures; −102, −150 and −196° C. The fracture elongation was in the maximum between −196 and −22° C, and increased as the test temperature increased from −196 to −50° C. This tendency of the temperature-dependence of elongation is similar to tha that of the percentage of the twin-related laths. The fracture elongation increases in the case where the occurrence of adjacent twin-related laths having the strain accommodation effect is frequently observed.

5. Conclusions

The orientation relationship between adjacent laths and the fracture elongation in the two-phase ($\alpha + \gamma$) Fe–Cr–Ni stainless steel were studied, and the following results were obtained:

(1) The peak temperature in 0°- and 45°-specimens was −50° C, and the peak elongation in a 90°-specimen appeared at both −102 and −50° C.

(2) There occurred a group of lath martensites within an original austenite grain. Both adjacent laths in a twin relationship and laths which were off a twin relationship were found out.

(3) The percentages of twin-related laths observed at −196° C, −150° C, −102° C and −50° C were 64, 67, 82 and 100%, respectively. This tendency agreed with the tendency of the increase of fracture elongation with increasing the temperature from −196 to −50° C, implying that the occurrence of twin-related laths aids the increase in elongation.

Acknowledgement

The authors would like to thank Dr Sadahiko Hirotzu for some valuable suggestions.

References

1. G. R. SPEICH and P. R. SWANN, *J. Iron Steel Inst.* **203** (1965) 480.
2. J. MARDER and A. R. MARDER, *Trans. ASM* **62** (1969) 1.
3. A. R. MARDER and G. KRAUSS, *ibid* **60** (1967) 651.
4. J. M. CHILTON, C. J. BARTON and G. R. SPEICH, *JISI* **209** (1970) 184.
5. C. A. APPLE, R. N. CARON and G. KRAUSS, *Met. Trans.* **5** (1974) 593.
6. Y. HIGO, F. LECROISEY and T. MORI, *Acta Met.* **22** (1974) 313.
7. G. KRAUSS and A. R. MARDER, *Met. Trans.* **2** (1971) 2343.
8. K. WAKASA and T. NAKAMURA, *Scripta Met.* **10** (1976) 129.
9. *Idem, J. Mater. Sci.* **12** (1977) 1438.
10. K. MATHIEU, *Arch. Eisenhüttenw.* **16** (1942) 215.
11. A. W. McREYNOLDS, *J. Appl. Phy.* **20** (1949) 896.
12. P. M. KELLY, *Acta Met.* **13** (1965) 635.

Received 6 October 1976 and accepted 27 January 1977.